

TECHNICAL NOTE

D-1186

INCOMPRESSIBLE NONVISCOUS BLADE-TO-BLADE FLOW THROUGH
A PUMP ROTOR WITH SPLITTER VANES

By James J. Kramer, Norbert O. Stockman, and Ralph J. Bean

Lewis Research Center
Cleveland, Ohio

NATIONAL AERONAUTICS AND SPACE ADMINISTRATION
WASHINGTON

April 1962

NATIONAL AERONAUTICS AND SPACE ADMINISTRATION

TECHNICAL NOTE D-1186

INCOMPRESSIBLE NONVISCOUS BLADE-TO-BLADE FLOW THROUGH

A PUMP ROTOR WITH SPLITTER VANES

By James J. Kramer, Norbert O. Stockman, and Ralph J. Bean

SUMMARY

The nonviscous flow through a mixed-flow pump impeller having one splitter vane between adjacent main blades has been analyzed on a blade-to-blade surface of revolution using a previously reported analysis method. Solutions were obtained for a variety of flow conditions including several cases in which whirl is imparted to the flow upstream of the impeller.

The velocity distributions on the main-blade surfaces and on the splitter-vane surfaces in the region of the splitter vane were strongly dependent on the assumed location of the rear stagnation points. Solutions were obtained by assuming values of slip factor and of division of flow around the splitter in addition to assuming the location of the rear stagnation points. These solutions indicated that the velocity distributions in the splitter-vane region are largely determined by the division of flow around the splitter vane and that only the region in the immediate vicinity of the trailing edge is affected by the slip factor.

Blade surface velocities were obtained from two approximate methods by specifying flow division and slip factor, and these results are compared with the more exact solutions of the analysis.

INTRODUCTION

In many instances in turbomachinery design, it is convenient to make use of splitter vanes in blade rows. Splitter vanes are partial blades that do not extend to the inlet of the machine. They are used often in pump designs with high ratios of fluid relative tangential velocity to axial velocity. For these cases, if the blade is to operate at small angles of attack, large inlet blade angles (measured from the axial direction) are required. Because of these large inlet angles, the thickness of the blades results in considerable blockage of the flow

area. This consideration limits the number of blades that can practically be used in the inlet region, particularly when low fluid velocity to minimize cavitation is a consideration.

Downstream of the inlet where the blades are more heavily loaded, it is generally necessary to have sufficient blades available so that the force per blade or blade loading is not excessive. The force on each blade is caused by the pressure difference across the blade and, hence, the velocity difference from blade to blade. If reasonably low inlet and outlet velocities are to be maintained, high blade loadings are to be avoided in order to avoid large negative blade surface velocity gradients that are conducive to boundary-layer separation. Frequently, the minimum number of blades sufficient for this purpose is greater than the number of blades desirable at the inlet from blockage considerations.

In order to resolve this difficulty, one or more splitter vanes can be inserted between adjacent full blades. These vanes decrease the loading per blade in the rearward part of the rotor without decreasing the available flow area at the inlet. In addition, splitter vanes tend to increase the total loading as evidenced by increased slip factors. As a result, a higher head rise can be attained with splitter vanes than without for the same rotative speed. Hence, if splitter vanes can be designed such that these advantages are gained without incurring excessive loss, then the use of splitter vanes would be a desirable additional degree of freedom in turbomachinery design.

Some of the possible sources of loss incurred by the introduction of splitter vanes are: (1) friction on the additional wetted area introduced by the splitter vanes; (2) velocity gradients on the splitter-vane surfaces conducive to separation; and (3) mixing downstream of the rotor caused by the vane wake and by uneven splitting of the flow by the splitter vane. Hence, the use of splitter vanes must result in an increase in efficiency of operation of the main blades such that a net overall gain in performance is accomplished. Whether such a net gain will be accomplished depends on the ability to design the splitter-vane shape and location so that it reduces the loading on the main blade, splits the mass flow in the manner desired, and results in acceptable velocity distributions on the blade surfaces.

The development of such design control in pumps is dependent on obtaining a better understanding of the flow through a blade row with splitter vanes. As an aid in this understanding, solutions of the non-viscous blade-to-blade flow in a typical pump impeller are desirable. In reference 1, a method was presented for analyzing the flow in a pump rotor with splitter vanes. The method of reference 1 yields the non-viscous incompressible blade-to-blade flow in a blade row with splitter vanes for any value of weight flow, rotational speed, and inlet whirl.

In order to obtain solutions with this method, however, the location of the rear stagnation point must be known or assumed.

In this report, the method of reference 1 is used to obtain solutions of the flow in a typical mixed-flow pump rotor having one splitter vane between adjacent main blades. The purpose here is to demonstrate the potentialities and limitations of the method of solution and to demonstrate the effect on the velocity distributions caused by the insertion of splitter vanes.

The results of applying the method of reference 1 to this pump rotor without the splitter vanes were presented in reference 2. By comparing the results of this report with the results of reference 2, the effect of the insertion of splitter vanes can be determined. Solutions were obtained for the same inlet flow conditions as for reference 2. Thus, a range of angle of attack is covered, and some cases with prewhirl (both positive and negative) are presented. The results are presented in detailed contour plots of flow properties for the design case, blade surface velocity plots for the off-design cases, and slip factors. The results of two approximate methods of analysis are compared with the exact-solution results. The sensitivity of the exact solutions to the assumed location of the rear stagnation point is investigated.

ANALYSIS

Equations and Boundary Conditions

The method of reference 1 was used to analyze the flow on a blade-to-blade surface through an impeller of the same geometry as that of reference 2, except that one splitter vane was inserted in each flow passage between blades. Thus, the rotor has eight full blades and eight splitter vanes. Two views of the impeller are shown in figures 1 and 2. The splitter vanes have the same camber-line shape as the main blades at corresponding axial stations. The mean camber line of the splitter vane was circumferentially equidistant from the main blades. This placement of the vanes is the most common practice in impeller design. At the leading edge of the splitter vane, the splitter-vane mean-camber-line direction and the flow direction in the impeller without splitter vanes differed by less than 0.5° for the design case.

The equation governing the flow process expressed in terms of the stream function ψ is

$$\left(\frac{1 + \lambda^2}{r^2} \right) \frac{\partial^2 \psi}{\partial \theta^2} + \frac{\partial^2 \psi}{\partial z^2} + \left(\frac{\lambda}{r} - \frac{\partial \ln b}{\partial z} \right) \frac{\partial \psi}{\partial z} = 2\lambda \omega b \quad (1)$$

where ψ is defined by

$$\left. \begin{aligned} \frac{\partial \psi}{\partial z} &= -bw_{\theta} \\ \frac{\partial \psi}{\partial \theta} &= rbw_z \end{aligned} \right\} \quad (2)$$

(All symbols are defined in the appendix.) Equation (1) is derived in reference 3 for flow along a stream sheet that is a surface of revolution. The derivatives with respect to z are understood to be the same as the boldfaced derivatives with respect to z of reference 3. The analysis method of reference 1 constructs solutions Ψ from linear combinations of basic solutions, such that

$$\Psi = A_0\psi_0 + A_1\psi_1 + A_2\psi_2 + A_3\psi_3 + A_4\psi_4 \quad (3)$$

The boundary conditions for the basic solutions are shown in table I.

The coefficients A_i of equation (3) are obtained from the solution of five linear equations in the A_i that express the boundary conditions of the solution of interest. The five equations are:

$$A_1 + A_2 + A_3 + A_4 = 1.0 \quad (4)$$

$$A_0 = \frac{1}{\omega_0} \left(\frac{\omega}{V} \right) = \frac{1}{\omega_0} X \left(\frac{\omega}{V} \right)_{\text{des}} \quad (5)$$

$$\sum_{i=0}^4 A_i \left(\frac{\partial \psi_i}{\partial z} \right)_u = \frac{-b_u(v_{\theta,u} - \omega r_u)}{V} = b_u r_u X(1 - Y) \left(\frac{\omega}{V} \right)_{\text{des}} \quad (6)$$

$$\sum_{i=0}^4 A_i \left(\frac{\partial \psi_i}{\partial z} \right)_{st,bl} = 0 \quad (7)$$

$$\sum_{i=0}^4 A_i \left(\frac{\partial \psi_i}{\partial z} \right)_{st,sp} = 0 \quad (8)$$

Equations (4) to (7) are similar to equations (6) to (9), respectively, of reference 2; and equation (8) specifies the location of the rear stagnation point on the splitter vane in the same way that equation (7) specifies the rear stagnation point on the full blade. The rear stagnation point on the splitter vane was originally assumed to occur at the blade tip (maximum z value, the point labeled A in fig. 2).

The stream surface geometry is the same as that of reference 2. This geometry is expressed by equations (1) and (2) of reference 2. The numerical procedure for obtaining the basic solutions was similar to that of reference 2. A similar grid was used, as shown in figure 2 for the region between the blades.

Cases Considered

The controlling parameters of the solution are the flow-rate parameter X defined as

$$X = \frac{\omega}{V} / \left(\frac{\omega}{V} \right)_{\text{des}}$$

and the prewhirl parameter Y defined as

$$Y = v_{\theta,u} / \omega r_u$$

where $(\omega/V)_{\text{des}}$ is 7412 radians per cubic foot and r_u is 2.9865 inches. Specification of the values of X and Y determines the flow for a given rear-stagnation-point location. Solutions were constructed for the same values of X and Y as was done in reference 2. Thus, results are available for flow through the same impeller at the same operating conditions with and without splitter vanes.

The specified conditions for the various cases considered are presented in table II. In the first five columns are the specified values of X and Y and the resultant values of angle of attack α , inlet flow angle β_i , and the upstream relative velocity ratio $w_u/\omega r_t$. The angle of attack is defined as the angle between the tangent to the blade camber line and the mean flow direction, computed on the basis of the one-dimensional continuity equation with the flow area based on the blade blockage at $z = 0.08$. Cases A to D are for no prewhirl with varying angle of attack. Case E has negative prewhirl, and cases F and G have positive prewhirl. For cases A to G the rear stagnation points occur at the blade and vane tips, the points labeled A in figure 2. In cases J to M, various assumptions for boundary conditions are made instead of assuming the locations of the rear stagnation points.

RESULTS AND DISCUSSION

The results of this report are presented in four categories: (1) contour plots of the stream function, velocity parameter, and static head parameter for the design flow condition; (2) blade surface velocities for several flow conditions; (3) investigation of the sensitivity of solutions to the location of the rear stagnation point; and (4) comparison of the results of approximate methods with the more exact results obtained herein.

Some of the results are summarized in table II, where values are listed for f_s and Ψ_{sp} . The slip factor f_s is defined as the ratio of the absolute tangential velocity of the fluid at the outlet of the blade row to the ideal absolute tangential velocity; that is, the absolute tangential velocity the fluid would have assuming the outlet flow direction equal to the outlet blade direction. In computing the ideal velocity, the blade thickness of 0.157 inch and splitter-vane thickness of 0.181 inch occurring at $z = 3.70$ is taken into account in determining flow area. The value of the stream function on the splitter-vane Ψ_{sp} indicates how the flow is divided around the splitter vane. The stream function Ψ varies from 0 to 1 across the passage from the driving to the trailing face.

Design Flow Case

In figure 3 are plotted contours of constant stream function or streamlines for the design flow case A. These contours are plotted on a projection of the stream surface on a plane such that distances in the z and θ directions are preserved. Angles are distorted. The tick marks at $\theta = 1.5$ indicate the line of zero angular distortion. Distortion increases with distance from that line. Results are shown for the rotor with splitter vanes in figure 3(a), and the results for the rotor without splitter vanes for the same flow conditions are reproduced from reference 2 in figure 3(b).

The most interesting aspect of the flow demonstrated by figure 3(a) is the division of the flow on either side of the splitter vane. The value of Ψ on the splitter vane is 0.56, which indicates that, although the splitter vane is located midway between main blades, 56 percent of the total flow passes between the driving face of the main blade and the splitter vane. In view of the consideration that the main-blade loading tends to shift the flow toward the trailing face, it might be expected that less than 50 percent of the flow would move between the driving face and the splitter vane. The leading edge of the splitter vane intercepts the $\Psi \approx 0.42$ for the flow solution of this impeller without splitter vanes (as shown in fig. 3(b)). Thus, if the splitter vane had zero

thickness and produced no distortion of the streamlines upstream of the splitter vane, the value of the stream function would be approximately 0.42.

However, when the splitter vane is inserted, the general trend expected is for the head rise of the rotor to increase by virtue of the increased solidity over that of the blade row without splitter vanes. This increase in head rise is indicated by an increased slip factor and is brought about by an increase in total blade loading. The increase in total blade loading was expected to be brought about by a decrease in main-blade loading and an increase in splitter-vane loading (from zero) that would more than balance the decrease in main-blade loading. The change in main-blade loading and the appearance of splitter-vane loading were expected to result in a shifting of the flow from the trailing face towards the driving face. For this rotor geometry and operating conditions, the value of Ψ_{sp} that resulted was 0.56.

The effect of the splitter vane in providing better guidance to the outlet flow is evidenced by the increased slip factor ($f_s = 1.01$, table II) compared with the no-splitter case. Thus, a sizable increase in head rise at the same flow rate and tip speed will be obtained.

The contours of velocity parameter for case A are shown in figure 4. The velocity parameter is the relative fluid velocity divided by the tip speed of the impeller. The results for the rotor without splitter vanes (ref. 2) are shown in figure 4(b). The velocity contours reflect the unequal flow split by showing high velocities in the passage between the splitter vane and the blade driving face. Upstream of the splitter vane the flow velocities are the same as for the case of the blade row without splitter vanes up to a θ of about 1.5 radians. This is a distance from the splitter-vane leading edge of three times the circumferential distance between the splitter vane and the main blade at the splitter-vane leading edge. The maximum velocity ratio on the vane leading edge is 0.57 with little deceleration on the vane trailing face.

Figure 5 displays contours of constant static head parameter for the blade row with and without splitter vanes. The static head parameter is defined as the difference between the local static head and the static head far upstream divided by $(\omega r_t)^2/2g$. The effect of the increased velocity in the blade driving surface channel on static head is evidenced by the low values of static head parameter on the driving face of the blade compared with the no-splitter-vane case. The reduction in driving surface head was sufficient to essentially unload the main blade in the splitter-vane region. This result is indicated by the nearly equal values of static head parameter at equal values of z (and therefore r) on the driving and trailing faces of the main blade in this region.

Some of the details of the flow for the design case such as the slip factor slightly greater than unity, the value of V_{sp} , and the unloading of the main blade in the splitter-vane region were somewhat unexpected by the authors. However, there were no experimental data to guide intuition in this area. In the following section, results are discussed for several off-design cases in which particular attention will be paid to the variation in the parameters just mentioned with angle of attack.

Off-Design Cases

The purpose of this section is to discuss how the flow responds to changes in the upstream flow conditions as caused by changes in the parameters X and Y . Results are presented for some off-design cases with various values for angle of attack and prewhirl.

Variation with angle of attack. - In figure 6 blade surface velocities are shown for the four cases B, A, C, and D in which the parameter X , and therefore angle of attack α , is varied. These cases have the same operating conditions as the cases so lettered in reference 2.

Comparison of the results shown in figure 6 with the corresponding results shown in reference 2 reveals that the blade surface velocities upstream of s equal to 0.40 on the driving face and 0.63 on the trailing face of the main blade do not differ from the corresponding results for the impeller without splitter vanes. The main-blade loading, however, is markedly reduced in the region of the splitter vane.

The splitter vane has a velocity distribution in the leading-edge region similar to that for a main blade operating at a positive angle of attack; that is, the velocity reaches a local maximum in a relatively sharp peak on the trailing face of the splitter vane.

The general shape of the velocity profiles on the rearward part of the blade and on the splitter vane does not change greatly as α is varied. The splitter vane appears to behave as if a decrease in its angle of attack were occurring as α for the main blade is increased.

After the velocity peak on the splitter vane near the leading edge, the velocity on the splitter-vane trailing face remains higher than that on the blade trailing face. The velocity on the splitter-vane driving face is lower than that on the blade driving face. The result is that the splitter vane is more highly loaded than the blade in the vicinity of the splitter vane. However, this difference in loading tends to decrease as α increases. The high loading of the splitter vane is a manifestation of the same flow condition that resulted in the unexpected flow division around the splitter vanes.

For the blade row without splitter vanes (ref. 2), the flow conditions of case D resulted in negative velocities on the driving face of the blade from $s = 0.53$ to 0.93 . The results for the blade row with splitter vanes shown in figure 6(d) indicate that the negative velocities are eliminated on the driving face of the blade but that a small region of negative velocities occurs on the driving face of the splitter vane (from $s = 0.78$ to 0.94) at this angle of attack. Thus, splitter vanes can be effective in reducing the tendency toward eddy formation at high loadings.

The slip factor decreased from 1.06 for case B to 0.91 for case D as a result of increasing X with Y constant. Increasing X corresponds to decreasing the volume flow rate for a fixed rotational speed. Hence, f_s decreases as the volume flow rate is decreased for a given value of rotational speed. This trend is the same as that for the blade row without splitter vanes.

The values of Ψ for the splitter-vane stagnation streamline are shown in table II in the column headed Ψ_{sp} . It can be noted that Ψ_{sp} is rather insensitive to changes in α for cases A to D.

Effects of prewhirl. - In figure 7(a) are displayed blade surface velocities for cases A, E, and F, for which $X = 1.0$ and values of prewhirl parameter Y are such as to result in angles of attack for cases E and F approximately equal to those for cases C and B, respectively. The results for cases E and F do not differ from the corresponding results for the blade row without splitter vanes upstream of s equal to 0.40 on the driving face and 0.63 on the trailing face. Hence, the same conclusions as cited in reference 2 concerning this region of the flow are valid.

Comparison of cases E and F with case A, all of which have the same value of X , reveals that the blade surface velocity changes resulting from changes in angle of attack while maintaining a constant-flow-rate parameter X are confined to the portion of the blade upstream of s equal to 0.30 on the trailing face and 0.08 on the driving face.

Blade surface velocities for case G are shown in figure 7(b). Case G has the same amount of negative prewhirl as case F, but with a larger value of X so as to result in a nearly zero angle of attack. The velocity profiles are similar to those for case A (same angle of attack) in the leading-edge region but show a larger main-blade loading in the region of the splitter vane.

Examination of table II for cases A, E, F, and G indicates that slip factor appears to be determined by the value of X rather than α for a fixed stagnation-point location.

Effect of Rear-Stagnation-Point Assumption

In reference 2, it was noted that the assumed location of the rear stagnation point had a considerable effect on the fluid velocities in the vicinity of the trailing edge and, hence, on the slip factor. In the case of a blade row with splitter vanes, the locations of two rear stagnation points must be assumed, which results in an increased uncertainty in the correspondence between the solution and the real flow through the impeller.

In the solutions presented thus far, the stagnation points were assumed to occur at the blade and vane tips; this is the assumption usually made in potential flow analyses. In the real fluid flow, the rear stagnation points do not occur because of the formation of blade wakes. Hence, it is not possible to obtain an experimental determination of the rear-stagnation-point locations.

In order to check the sensitivity of the solutions to the rear-stagnation-point assumption, case J was constructed. (The letters G, H, and I were not used in identifying the various cases in order to avoid confusion with cases G, H, and I of reference 2, for which no analogues occur in this report.) In case J the stagnation point on the splitter vane was assumed to occur at the point labeled J ($z = 3.71$) in figure 2. Point J is the grid point closest to the tip on the rounded trailing edge.

The rear stagnation point on the main blade was assumed to occur at the tip as in all previous cases. The blade surface velocities for case J are shown in figure 8(a). The results do not differ from those for case A upstream of s equal to 0.65 on the trailing face and 0.43 on the driving face. However, downstream of these points the results differ considerably. The loading on the main blade is increased over that for case A and exceeds the loading on the splitter vane in that region. This result is just opposite to that for case A. Also, the slip factor is reduced from 1.01 for case A to 0.90 for case J. The flow split is affected considerably as is evidenced by the change in value of the stream function on the splitter vane from 0.56 for case A to 0.45 for case J. It is thus apparent that a small change in the rear-stagnation-point location causes a significant change in the division of the flow, division of loading between vane and blade, and total loading (slip factor).

It was noted in reference 2 that the solutions for flow through the blade row without splitter vanes was affected near the blade outlet by the assumed location of the rear stagnation point. However, the effect is so drastic in the case of the blade row with splitter vanes as to render questionable the procedure of specifying the solutions by the specification of the rear stagnation points at the blade and vane tips.

Any two better understood physical conditions that result in independent relations among the Ψ_i can be substituted for the assumption of the locations of the rear stagnation points. Some examples of such physical conditions are the value of Ψ_{sp} and the value of f_s .

In order to investigate further the relations among Ψ_{sp} , f_s , and the division of loading between vane and blade, cases K, L, and M were constructed. In case K the rear-stagnation-point location on the main blade is the same as that for case A. However, instead of specifying the rear-stagnation-point location on the splitter vane, the stream function was specified to have the value 0.50 on the splitter vane. The resulting blade surface velocities are shown in figure 8(b). The loading on the splitter vane is nearly equal to the loading on the corresponding part of the main blade. The slip factor is 0.95.

Cases A, J, and K all have the same values of X and Y . They can be distinguished by their values of f_s and Ψ_{sp} . Case A has $f_s = 1.01$ and $\Psi_{sp} = 0.56$; case K has $f_s = 0.95$ and $\Psi_{sp} = 0.50$; and case J has values of 0.90 for f_s and 0.45 for Ψ_{sp} . For case A the loading on the splitter vane is considerably greater than that on the corresponding part of the main blade. For case K the loadings are nearly equal, and for case J the situation is the reverse of that for case A. Thus, at this point it is not known which of the two parameters, f_s and Ψ_{sp} , is related to the trend in the loading.

In order to decide this, two additional cases were constructed: case L in which f_s was specified as 0.90 and Ψ_{sp} as 0.50, and case M in which f_s is 0.95 and Ψ_{sp} is 0.45. Thus, cases K and L have $\Psi_{sp} = 0.50$, and cases J and M have $\Psi_{sp} = 0.45$. Cases K and L (figs. 8(b) and 9(a), respectively) have nearly the same velocity distribution except near the trailing edge. Similarly, cases J and M (figs. 8(a) and 9(b)) have the same velocity distribution except near the trailing edge. Thus, the specification of Ψ_{sp} appears to be the determining factor for the velocity distribution over the major part of the splitter vane and the main blade in the vicinity of the splitter vane. The effect of the specification of f_s is limited to the region $s > 0.80$ on the driving surface and $s > 0.92$ on the trailing surface for the cases considered.

It would be interesting to note the stagnation-point locations that result when the parameters f_s and Ψ_{sp} are prescribed as was done in cases K, L, and M. However, the determination of the exact location of the rear stagnation point is not practical because of the coarseness of the grid. It does appear that the stagnation points for cases K, L, and M fall between cases A and J, with case K closer to case A, and cases L and M closer to case J and very close to each other. The most probable

order, then, in moving from case A around the splitter tip to case J is A($\Psi_{sp} = 0.56$, $f = 1.01$), K(0.50, 0.95), L(0.50, 0.90), M(0.45, 0.95), and J(0.45, 0.90).

Comparison with Approximate Methods

The approximate methods of analysis reported in references 4 and 5 have been used to obtain blade surface velocities in impellers with splitter vanes. These methods were not originally designed for such applications. However, the assumption of a value for the division of the flow on either side of the splitter vane makes approximate analysis possible. These two methods are the same as commented on in reference 2, and are referred to as the circulation method (ref. 4) and the linear pressure method (ref. 5).

The results of these two approximate analysis methods are shown in figure 10 for the same values of f_s and Ψ_{sp} as for cases L and M. The blade surface velocities computed upstream of the splitter vane are the same as those for a blade row without splitter vanes. The reader is referred to reference 2 for a discussion of the comparison of results upstream of the splitter vane. In the vicinity of the splitter vane, the agreement between the results of both approximate methods and the results obtained using the exact method (fig. 9) is good. In both cases the approximate methods do not predict the gradual acceleration on the driving face of the blade beginning at $s = 0.48$. This transition region just ahead of the splitter vane is the region in which the approximate methods cannot be expected to yield good results because the flow in this area is strongly influenced by local geometry rather than the general shape of the channel. This region is similar to the regions near the leading and trailing edges in that respect.

For the linear pressure method results for case L, the surface velocities in the channel between the splitter and the driving face show minor deviations from those in the channel between the splitter and the trailing face, although the assumptions used in the method indicate that no difference should exist. These slight variations were caused by small changes in the flow area arising from variations in the fairing of the blade surface through the grid points.

SUMMARY OF RESULTS

The major results of the analysis of the flow through a pump impeller with splitter vanes are:

1. Comparison of flow through the impeller with and without splitter vanes reveals that the effect of the vanes is felt only a short distance

upstream of the leading edge of the vanes. Thus, the flow in the inlet region is unaffected by the insertion of splitter vanes. The conclusions concerning the flow in the inlet region are the same as those for the blade row without splitter vanes reported previously.

2. In the solutions where the stagnation points were assumed to occur at the blade tip, the effects of the splitter vanes were to increase slip factor and, hence, head rise and to retard the formation of the eddy on the driving face of the main blade at large positive angles of attack.

3. The assumed locations of the rear stagnation points significantly affected the flow division around the splitter, the slip factor, and the division of loading between the vane and the main blade.

4. The sensitivity of the results to the assumed location of the stagnation points indicates that an alternate means of specifying the solution is necessary in order to realize the maximum utility of this analysis method. Such an alternate means would consist of specifying some physical condition that can be determined experimentally.

5. When examples were computed with a specified value of the stream function on the splitter vane Ψ_{sp} and slip factor f_s , the specification of Ψ_{sp} was found to determine the magnitude of the loading on the blade and the splitter vane. The value of slip factor determined the blade surface velocities in the immediate vicinity of the trailing edge.

6. The results of the blade-to-blade analysis method were compared with the results of two approximate methods of analysis. The results were obtained from both exact and approximate methods for the same values of f_s and Ψ_{sp} . The agreement between the two methods of analysis is good except on the driving face of the main blade just ahead of the splitter vanes.

Lewis Research Center

National Aeronautics and Space Administration
Cleveland, Ohio, October 20, 1961

APPENDIX - SYMBOLS

The following symbols are used in this report:

A	coefficient of basic solution in linear combination
b	stream-sheet thickness in radial direction, in.
f_s	slip factor
g	acceleration due to gravity
H	total head
h	fluid static head
ΔH	head rise parameter, $\frac{H_o - H_i}{(\omega r_t)^2/g}$
r	radial distance from impeller axis, in.
s	fraction of total distance along blade surface from leading edge to rear stagnation point
V	volume flow rate through streamtube
v	absolute fluid velocity
w	fluid velocity relative to rotating impeller
X	parameter indicating fraction of design ratio of rotor angular velocity to volume flow, $\frac{\omega}{\bar{V}} / \left(\frac{\omega}{\bar{V}} \right)_{des}$
Y	prewhirl parameter, $v_{\theta,u}/\omega r_u$
z	axial distance from impeller inlet, in.
α	mean angle of attack, deg
β	mean flow angle, deg
θ	angular distance from an arbitrary radial line, radians
λ	dr/dz
Ψ	stream function for real solution defined by eq. (3)

ψ stream function for basic solution defined by eq. (2)

ω rotor angular velocity, radians/sec

Subscripts:

bl main blade

d downstream (fig. 1)

des design

i blade inlet

ideal having outlet flow direction equal to outlet blade direction

i,0,1, basic solution numbers
2,3,4

o blade outlet

sp splitter vane

st stagnation point

t impeller tip

u upstream (fig. 1)

z component in z-direction

θ component in θ -direction

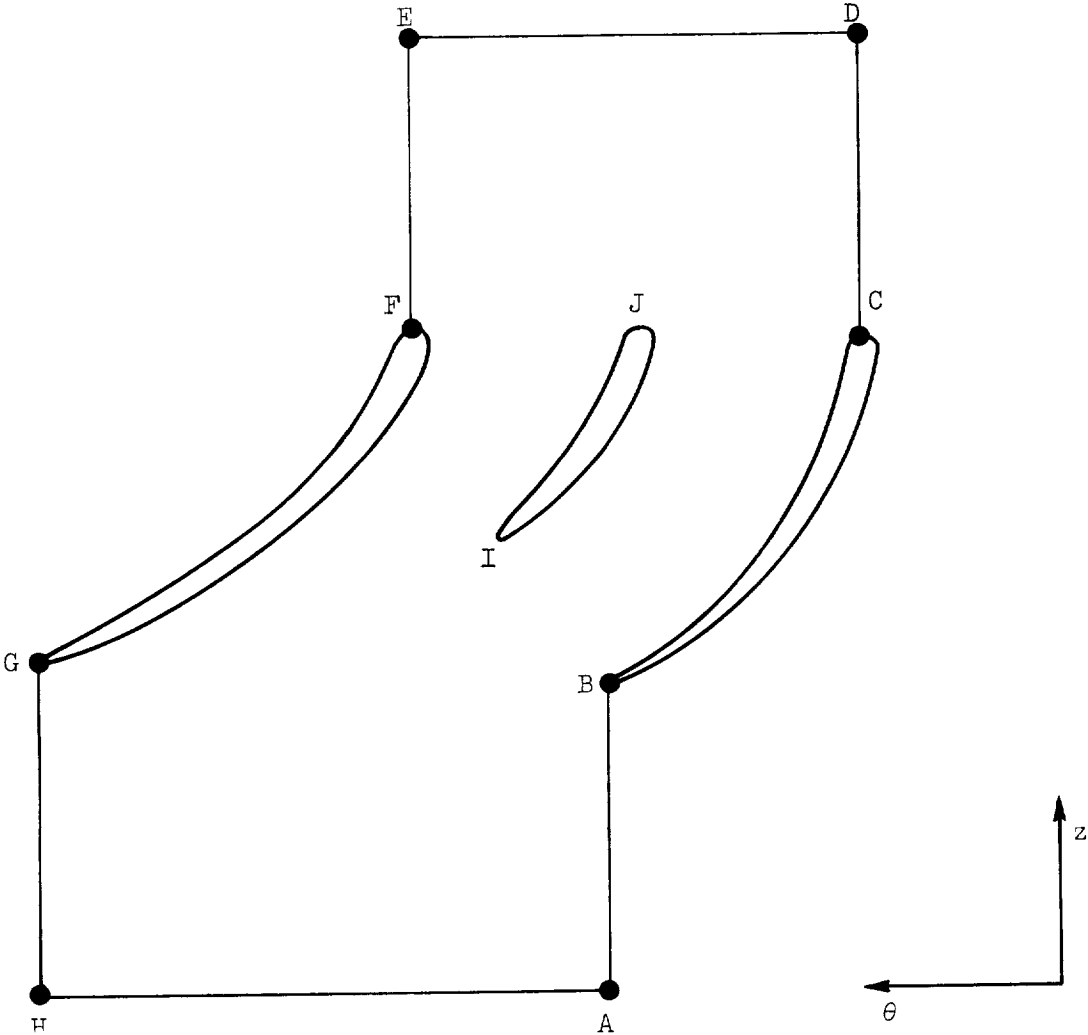
REFERENCES

1. Kramer, J. J.: Analysis of Incompressible, Nonviscous Blade-to-Blade Flow in Rotating Blade Rows. Trans. ASME, vol. 80, no. 1, Jan. 1958, pp. 236-275.
2. Kramer, J. J., Stockman, N. O., and Bean, R. J.: Nonviscous Flow Through a Pump Impeller on a Blade-to-Blade Surface of Revolution. NASA TN D-1108, 1961.
3. Wu, Chung-Hua: A General Theory of Three-Dimensional Flow in Subsonic and Supersonic Turbomachines of Axial-, Radial-, and Mixed-Flow Types. NACA TN 2604, 1952.

4. Stanitz, John D., and Prian, Vasily D.: A Rapid Approximate Method for Determining Velocity Distribution on Impeller Blades of Centrifugal Compressors. NACA TN 2421, 1951.
5. Hamrick, Joseph T., Ginsburg, Ambrose, and Osborn, Walter M.: Method of Analysis for Compressible Flow Through Mixed-Flow Centrifugal Impellers of Arbitrary Design. NACA Rep. 1082, 1952. (Supersedes NACA TN 2165.)

TABLE I. - BOUNDARY VALUES FOR BASIC SOLUTIONS

Basic solution	Boundary value of ψ							ω
	At A	At D	At E	At H	Along BC	Along FG	Along IJ	
0	0	0	0	0	0	0	0	ω_0
1	0	0	1	1	0	1	.6	0
2	0	1	2	1	0	1	.6	0
3	1	0	1	2	0	1	.6	0
4	0	0	1	1	0	1	.4	0



E-815

TABLE II. - SUMMARY OF SPECIFIED CONDITIONS AND
RESULTANT FLOW PROPERTIES

Case	X	Y	α	β_i	$\frac{w_u}{w r_t}$	f_s	Ψ_{sp}	ΔH	β_o
A	1.0	0	0°	-83°4'	0.62	1.01	0.56	0.734	40°20'
B	.8	0	-1°44'	-81°20'	.62	1.06	.56	.697	37°34'
C	1.33	0	1°43'	-84°47'	.62	.97	.56	.774	44°4'
D	4.0	0	5°9'	-88°15'	.62	.91	.57	.852	63°23'
E	1.0	-.3333	1°37'	-84°41'	.83	1.01	.56	.861	40°20'
F	1.0	.2	-1°35'	-81°29'	.50	1.01	.56	.656	40°20'
G	1.25	.2	0°6'	-83°10'	.50	.98	.56	.684	43°41'
J	1.0	0	0°	-83°4'	.62	.90	.45	.653	48°5'
K	1.0	0	0°	-83°4'	.62	.95	a.50	.692	44°3'
L	1.0	0	0°	-83°4'	.62	a.90	a.50	.652	48°10'
M	1.0	0	0°	-83°4'	.62	a.95	a.45	.690	44°39'

^aSpecified value.

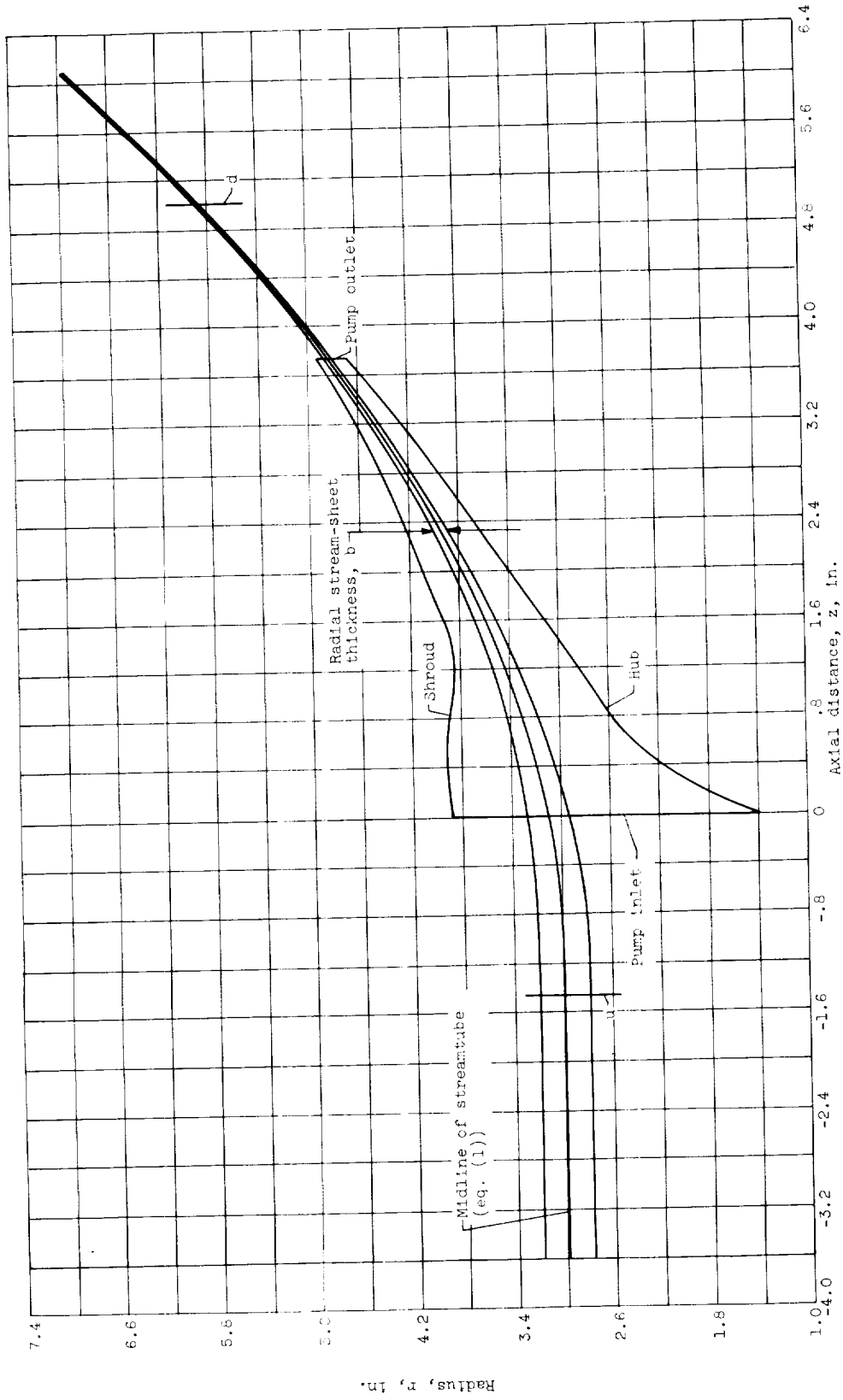


Figure 1. - Hub-shroud profile of pump showing meridional section of streamtube analyzed in this report.

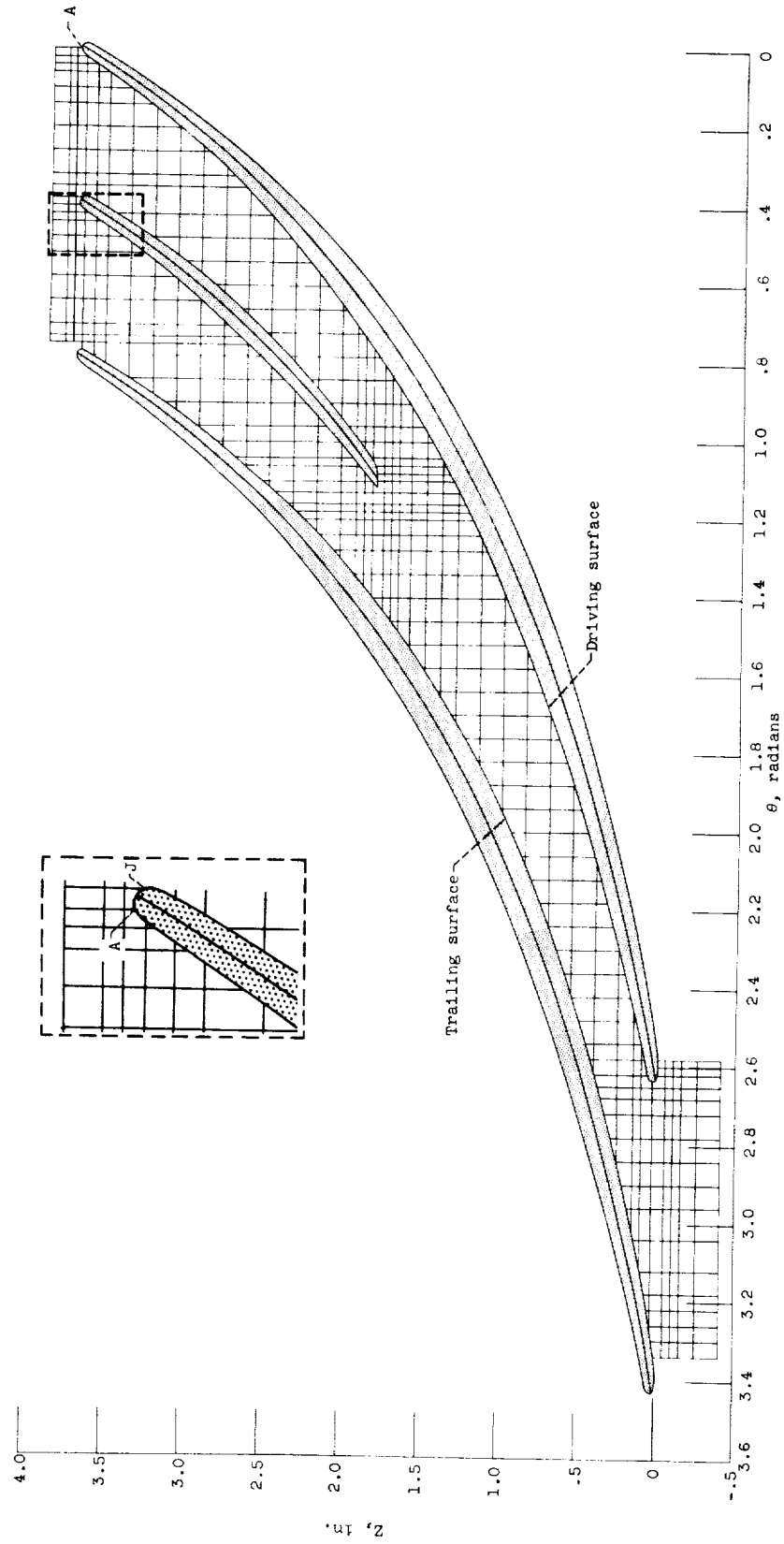


Figure 2. - Blade-to-blade section of streamtube showing grid used for numerical solution.

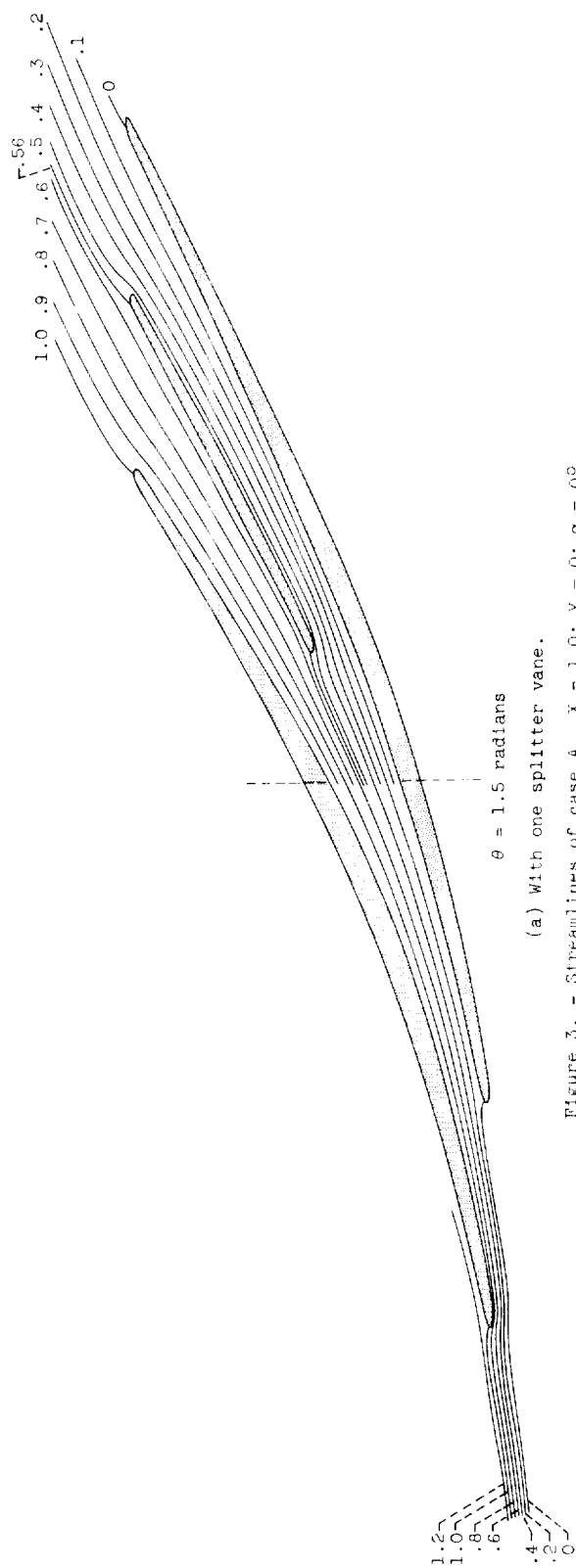
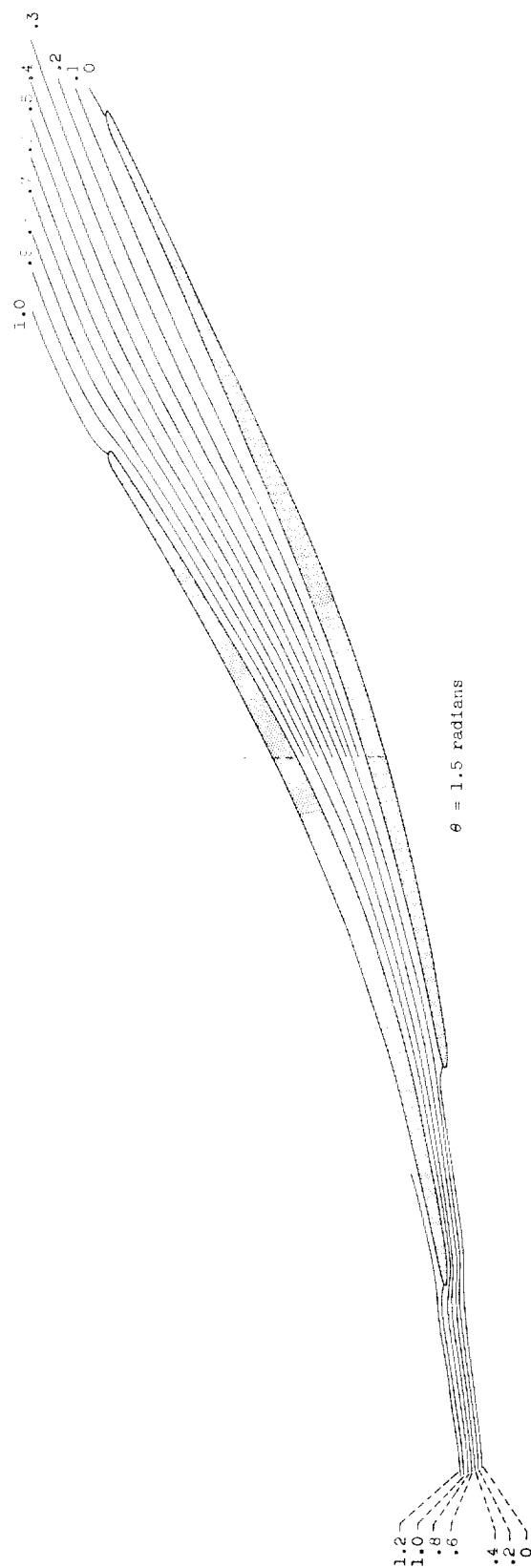


Figure 3. - Streamlines of case A. $X = 1.0$; $Y = 0$; $\alpha = 0^\circ$.



(b) Without splitter vane.

Figure 3. - Concluded. Streamlines of case A. $X = 1.0$; $Y = 0$; $\alpha = 0^\circ$.

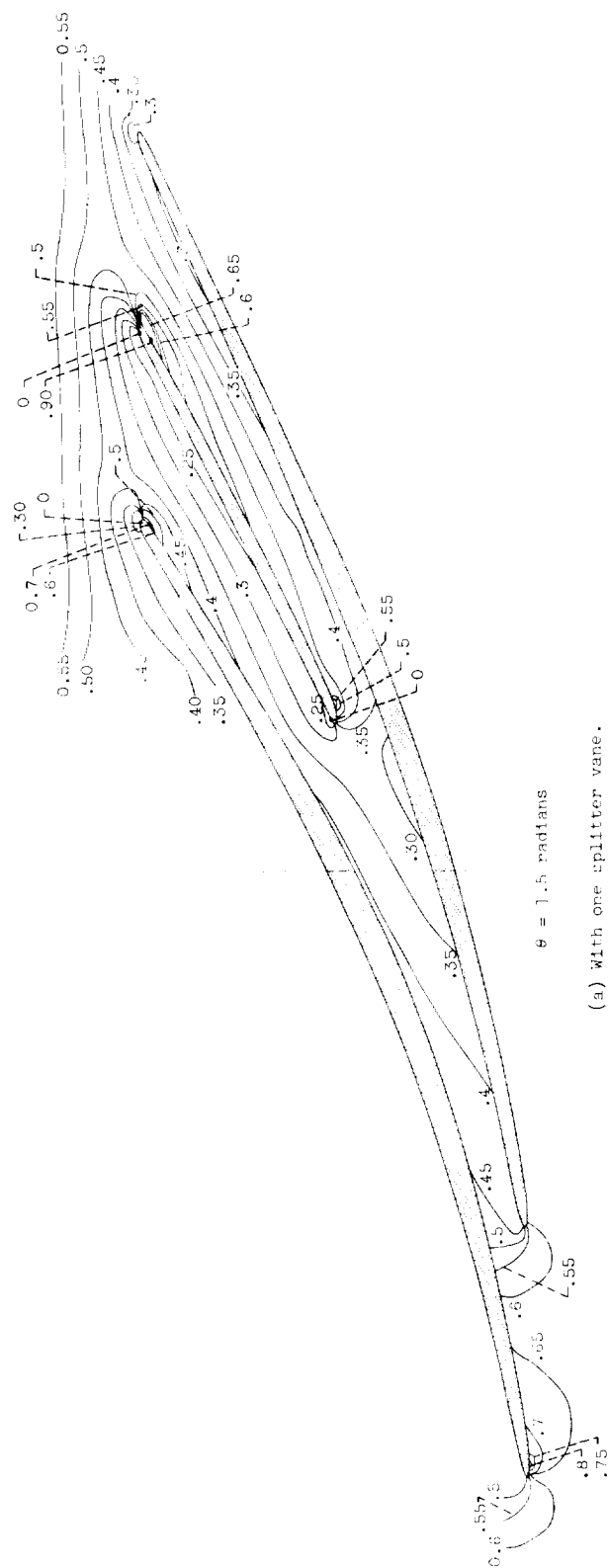
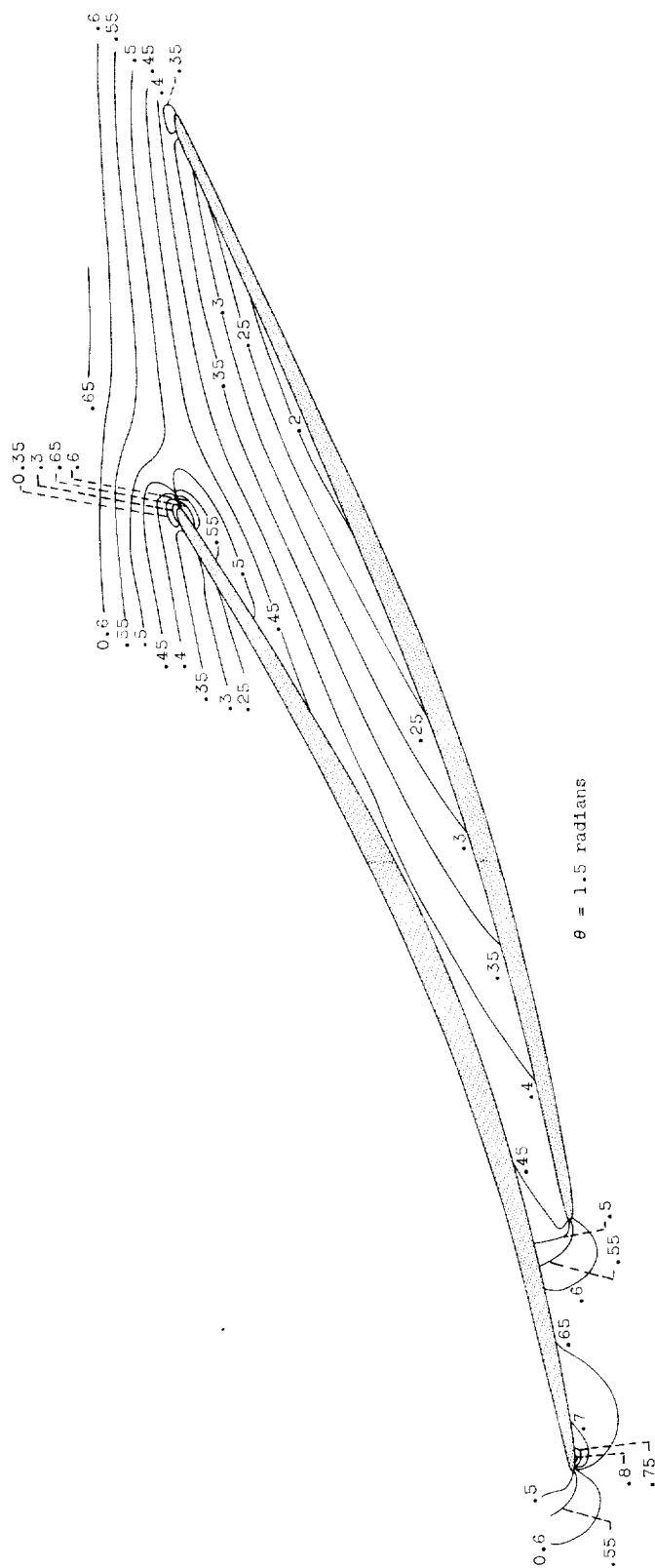
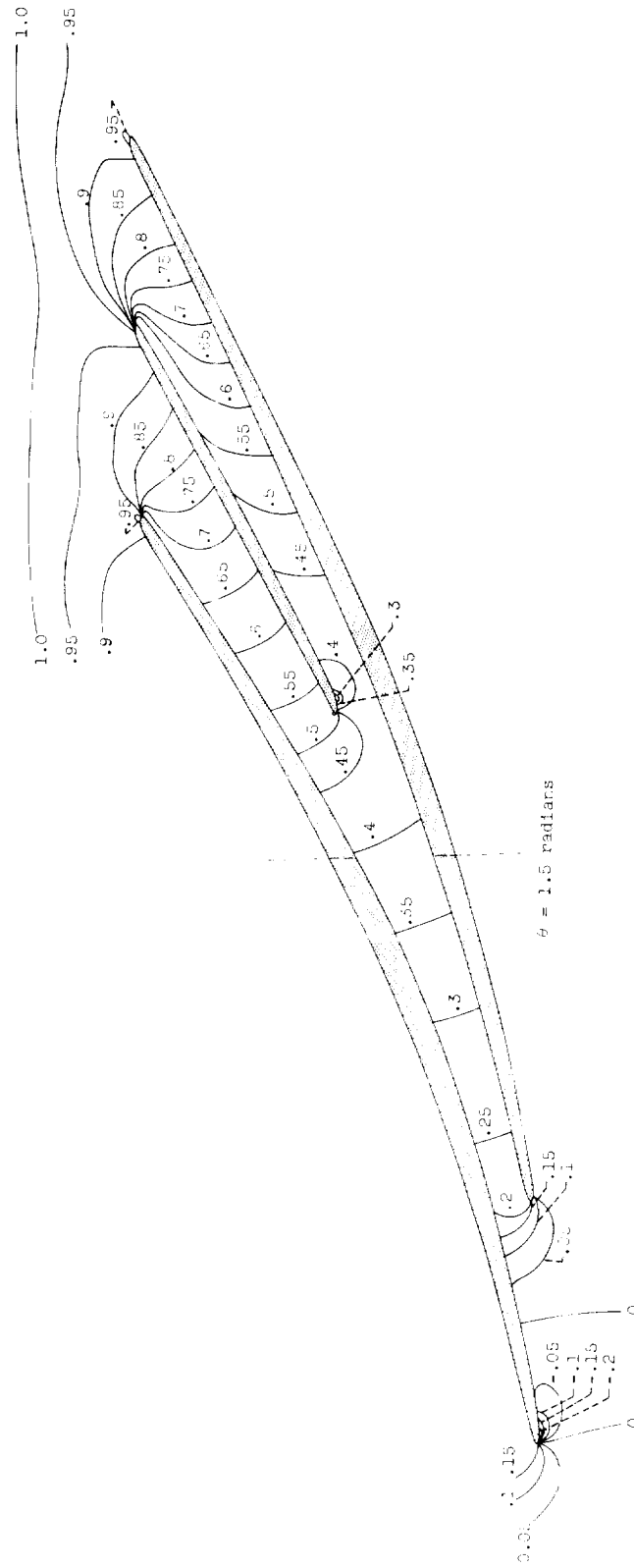


Figure 4. - Contours of constant relative velocity ratio of case A. $X = 1.0$; $Y = 0$; $\alpha = 0^\circ$.



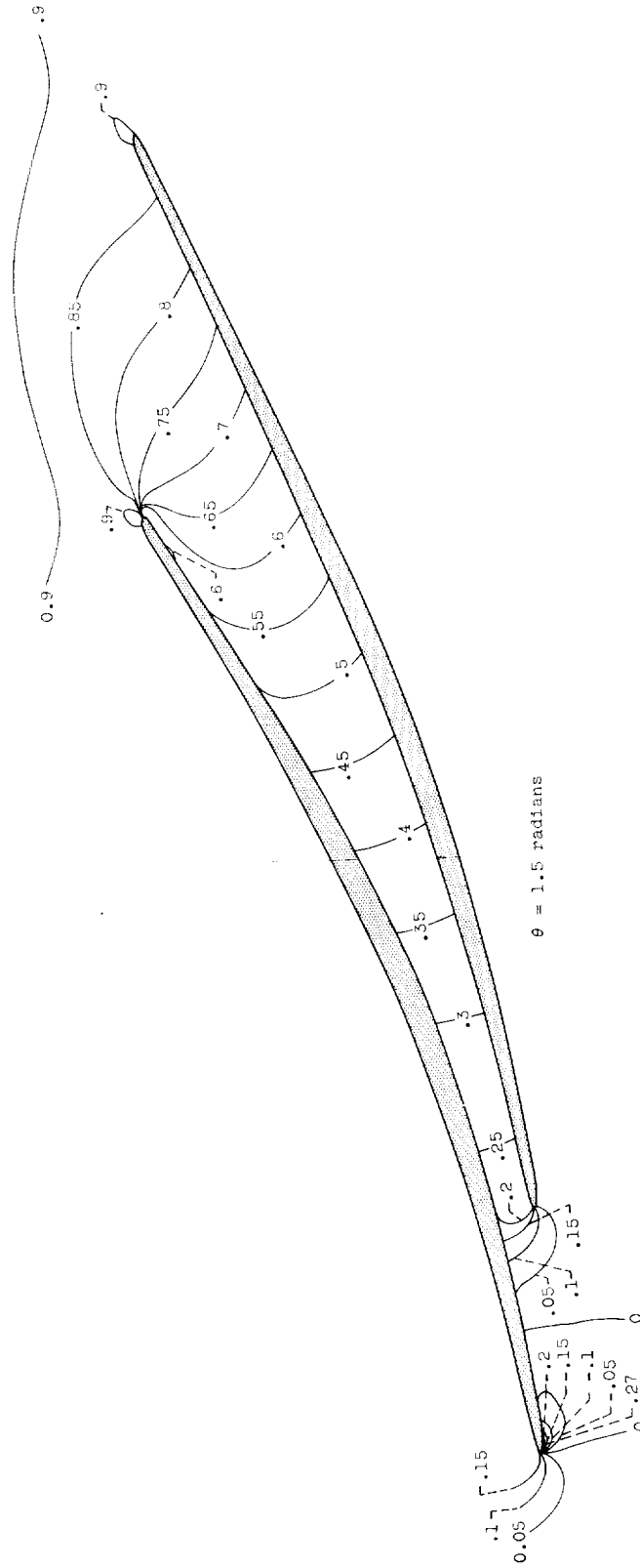
(b) Without splitter vane.

Figure 4. - Concluded. Contours of constant relative velocity ratio of case A. $X = 1.0$; $Y = 0$; $\alpha = 0^\circ$.



(a) With one splitter vane.

Figure 5. - Contours of constant static head parameter of case A. $X = 1.0$; $\gamma = 0$; $\alpha = 0^\circ$.



(b) Without splitter vane.

Figure 5. - Concluded. Contours of constant static head parameter of case A. $X = 1.0$; $Y = 0$; $\alpha = 0^\circ$.

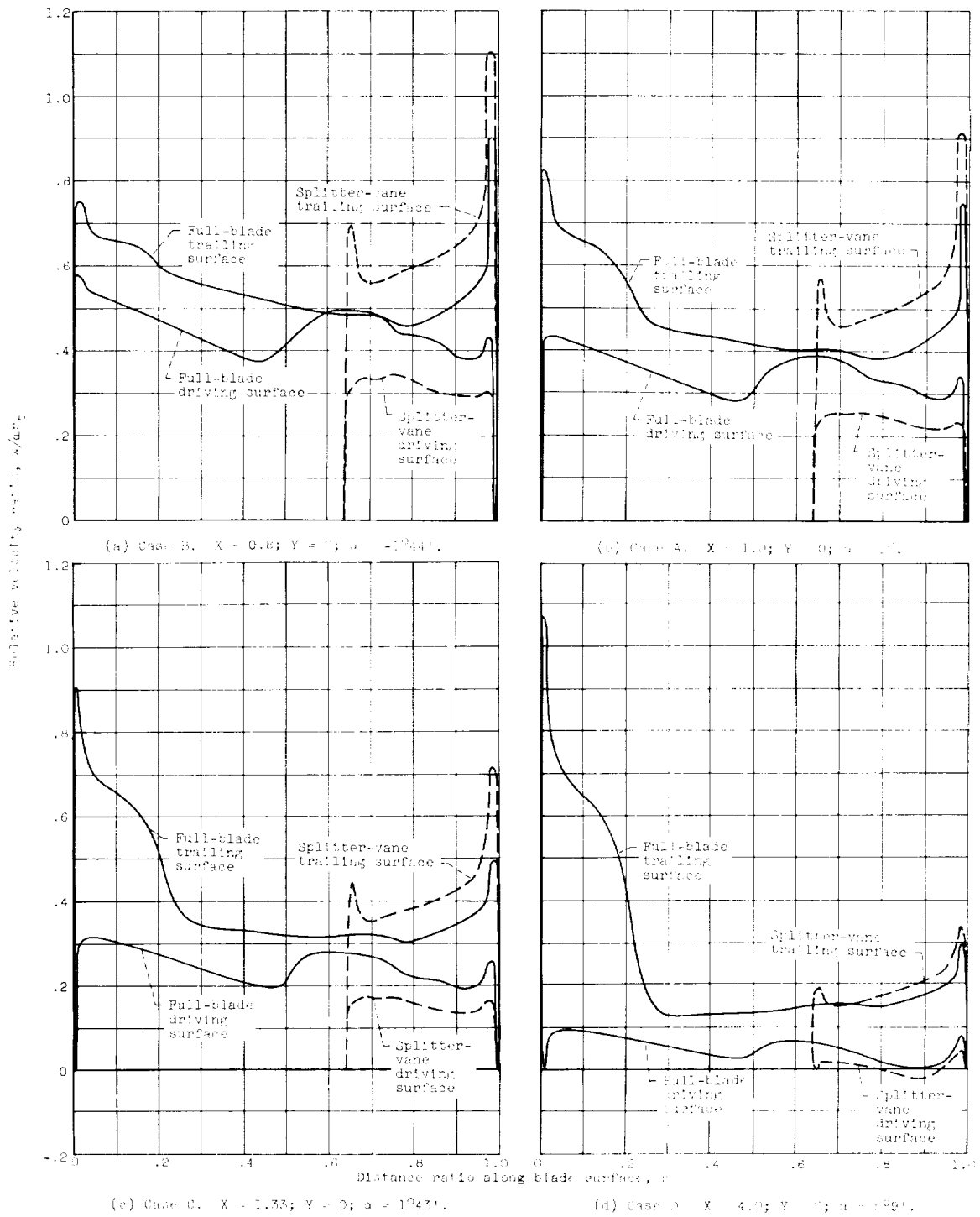
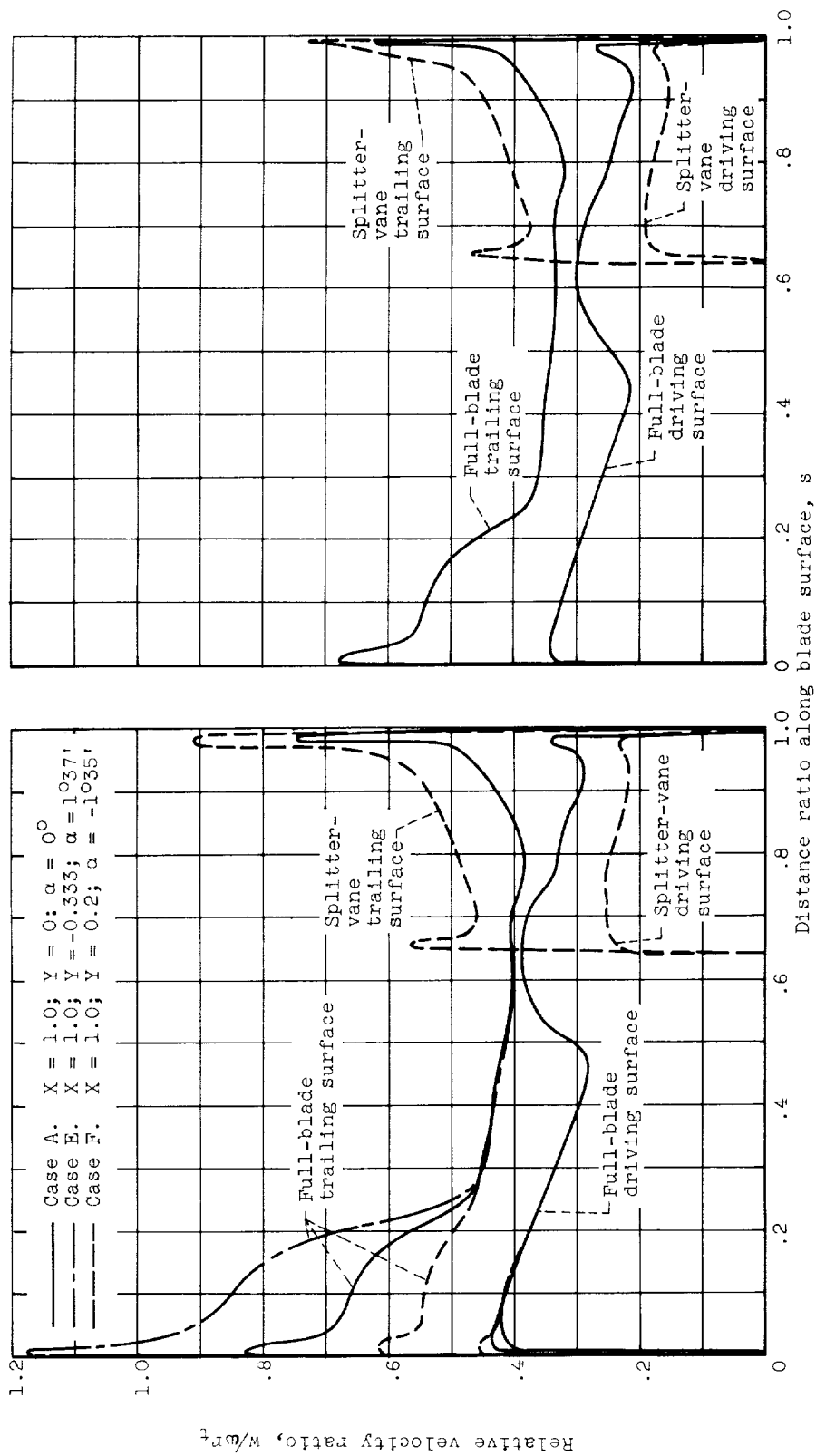
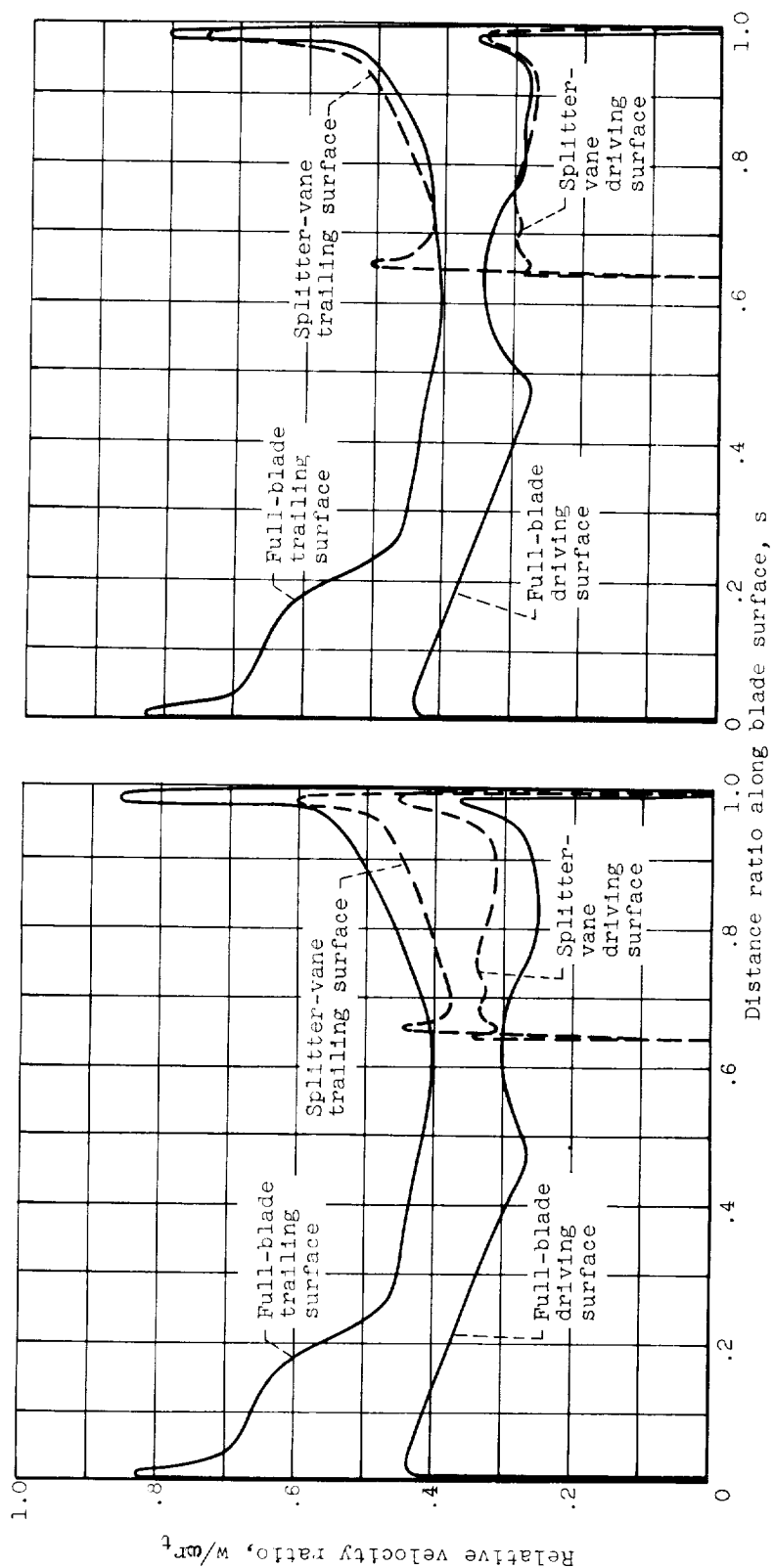


Figure 4. - Distribution of relative velocity ratio along blade surface for cases with no potential.



(a) Cases E ($\alpha = 1^\circ 37'$) and F ($\alpha = -1^\circ 35'$) compared with case A ($\alpha = 0^\circ$).

Figure 7. - Distribution of relative velocity ratio along blade surface for cases with nonzero prewhirl.



(a) Case J. $X = 1.0$; $Y = 0$; rear stagnation point on splitter vane located at point J (fig. 2).

(b) Case K. $X = 1.0$; $Y = 0$; $\psi_{sp} = 0.50$.

Figure 8. - Distribution of relative velocity ratio along blade surface showing effect of changing boundary condition on the splitter vane.

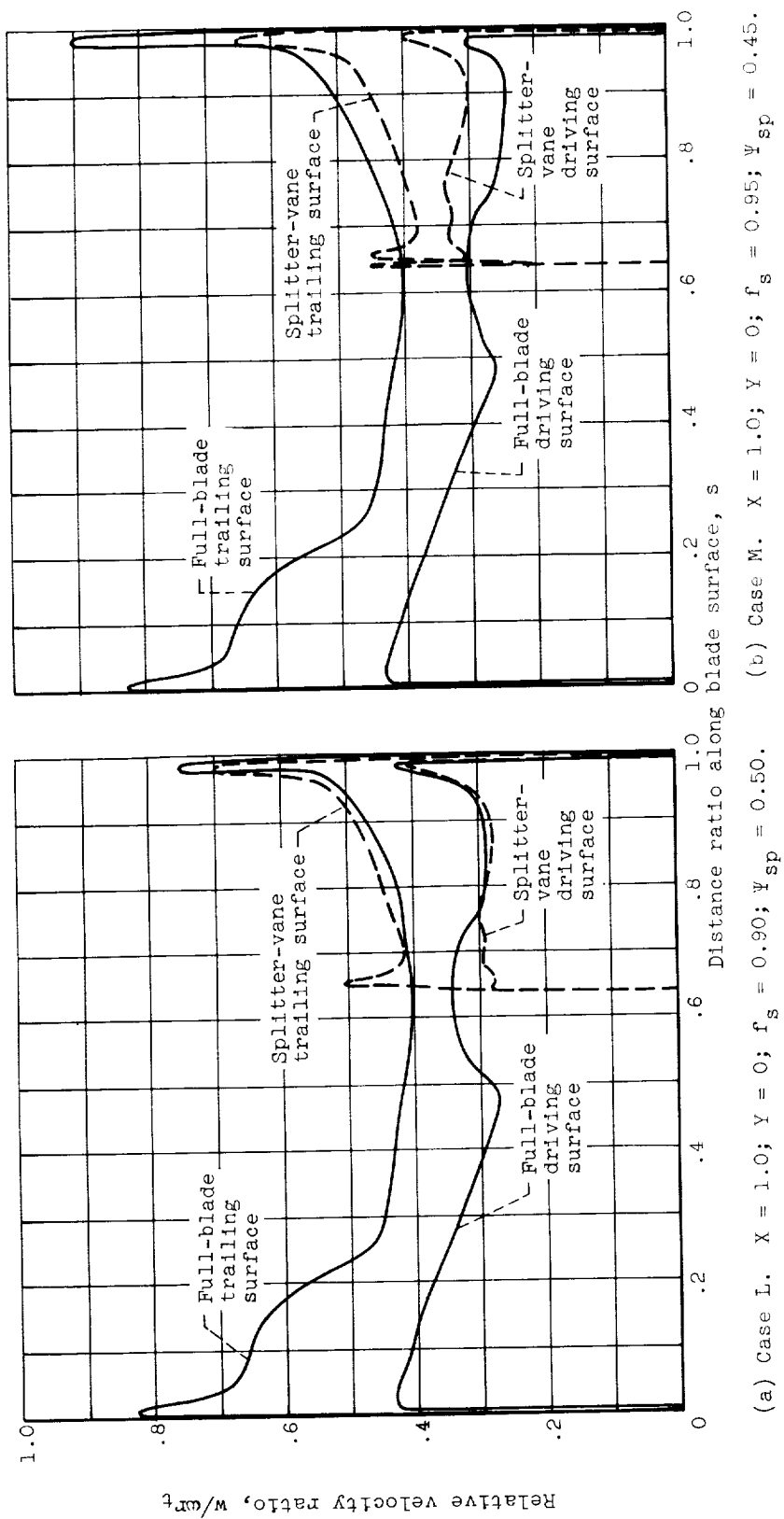


Figure 9. - Distribution of relative velocity ratio along blade surfaces for cases obtained by specifying slip factor and flow split.

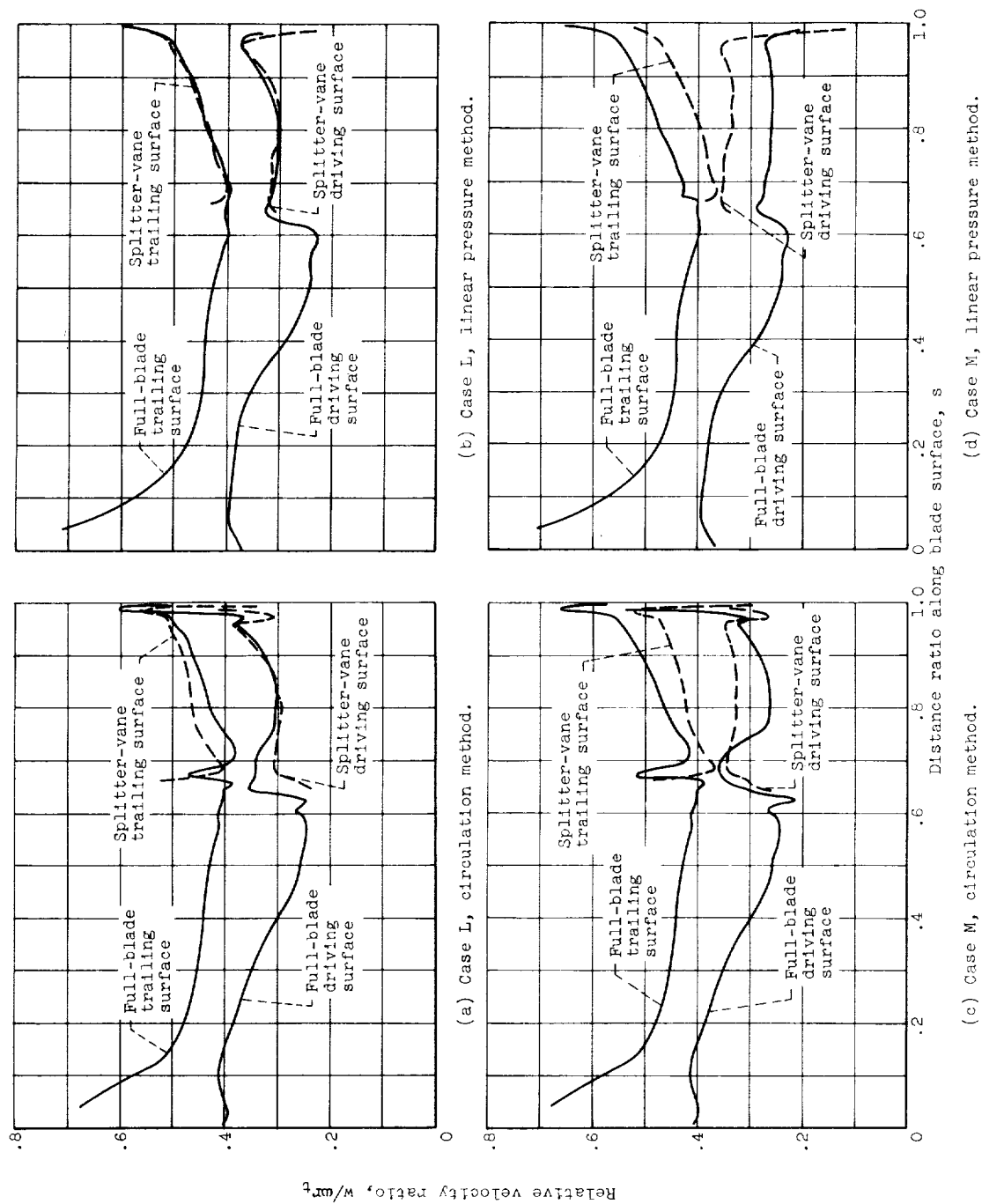


Figure 10. - Distribution of relative velocity ratio along blade surface obtained by approximate methods.